Journal of Nuclear Medicine, published on September 16, 2021 as doi:10.2967/jnumed.121.262530

Epidermal growth factor receptor targeted fluorescence molecular imaging for postoperative lymph node assessment in patients with oral cancer

Running title: Fluorescence assessment of lymph nodes

Jasper Vonk[1]*, Jaron G. de Wit[1]*, Floris J. Voskuil[1,3], Yang Hang Tang[1], Wouter T.R. Hooghiemstra[2], Matthijs D. Linssen[2], Evert van den Broek[3], Jan J. Doff[3], Sebastiaan A.H.J. de Visscher[1], Kees-Pieter Schepman[1], Bert van der Vegt[3], Gooitzen M. van Dam[4,5], Max J.H. Witjes[1]

*Both authors contributed equally to this work and therefore share first authorship

Affiliations:

1. Department of Oral & Maxillofacial Surgery, University of Groningen, University Medical Center Groningen, the Netherlands
2. Department of Clinical Pharmacy and Pharmacology, University Medical Center Groningen, The Netherlands
3. Department of Pathology & Medical Biology, University of Groningen, University Medical Center Groningen, the Netherlands
4. Department of Nuclear Medicine and Molecular Imaging and Medical Imaging Center, University of Groningen, University Medical Center Groningen, the Netherlands
5. TRACER BV, Groningen, The Netherlands

Correspondence: Dr. M.J.H. Witjes, Department of Oral & Maxillofacial Surgery, University Medical Center Groningen, PO Box 30.001, 9700 RB Groningen the Netherlands. E-mail: m.j.h.witjes@umcg.nl, phone: +31 50 361 13841, fax: +31 50 361 12831

Word count: 5041

ABSTRACT

Rationale: In most oral cancer patients, surgical treatment includes resection of the primary tumor combined with the excision of lymph nodes (LN)s, either for staging or treatment. All LNs harvested during surgery require tissue processing and subsequent microscopic histopathological assessment to determine the nodal stage. In this study, we investigated the use of the fluorescent tracer cetuximab-800CW to discriminate between tumor-positive and tumor-negative LNs before histopathological examination.

Methods: Here, we report a retrospective ad hoc analysis of a clinical trial designed for resection margin evaluation of oral squamous cell carcinoma patients (NCT02415881). Two days prior to surgery, patients were intravenously administered with 75 mg cetuximab followed by 15 mg cetuximab-800CW, an Epidermal Growth Factor Receptor (EGFR)-targeting fluorescent tracer. Fluorescence images were obtained of excised, formalin-fixed LNs and correlated with histopathological assessment.

Results: Fluorescence molecular imaging of 514 LNs (61 pathologically positive nodes) can detect tumor-positive LNs *ex vivo* with 100% sensitivity and 86.8% specificity (AUC 0.97). In this cohort, the number of LNs that require microscopic assessment was decreased by 77.4%, without missing any metastasis. Additionally, in 7.5% of the fluorescence false-positive LNs, we identified metastases missed by standard histopathological analysis.

Conclusion: Our findings suggest that EGFR-targeted fluorescence molecular imaging can aid in the detection of LN metastases in the *ex vivo* setting in oral cancer patients. This image-guided concept can improve the efficacy of postoperative LN examination and identify additional metastases, which safeguards appropriate postoperative therapy and may improve patient prognosis.

Key Words: Fluorescence molecular imaging, Lymph node metastasis, Cetuximab-800CW, Epidermal Growth Factor Receptor, Head and Neck Cancer

INTRODUCTION

In oral squamous cell carcinoma (OSCC), the presence of lymph node (LN) metastasis has a major impact on prognosis and is associated with a significantly reduced survival *(1, 2)*. Consequently, assessment of LN status is important for determining the postoperative treatment strategy of the neck and consists of clinical assessment and preoperative radiographic imaging (i.e. magnetic resonance imaging, computed tomography or ultrasound). If clinically suspicious LNs (cN+) are identified, a therapeutic neck dissection is indicated. However, even for a clinically node-negative neck (cN0), an elective neck dissection or sentinel node is widely performed for staging as up to 30% of these patients have occult LN (micro-)metastases *(3, 4)*. Postoperatively, the neck dissection specimen is macroscopically analyzed by the pathologist for the presence of LNs *(5)*, and all LNs are sectioned and stained with H&E or cytokeratin for microscopic evaluation. Other techniques for identifying LN metastasis are not clinically available yet. It, therefore, is interesting to explore other methods to identify metastasis in LNs, especially when the tissue is intact, prior to routine processing.

Fluorescence molecular imaging (FMI), especially in the near-infrared window, is a rapidly evolving imaging technique in surgical oncology *(6)*. FMI can provide real-time information on subsurface tissue by visualizing tumor-specific contrast agents *(7)*, particularly when a controlled imaging environment is ensured *(8)*. An interesting target for FMI is the Epidermal Growth Factor Receptor (EGFR), which is overexpressed in up to 90% of OSCC *(9)*. Several phase I studies have shown the potential of EGFR-targeted FMI for intraoperative *ex vivo* tumor margin assessment in OSCC *(10, 11, 12)*. However, little is known about EGFR-targeted imaging and identification of OSCC metastasis in LNs. FMI may allow for simultaneous *ex vivo* assessment of LN status when a neck dissection is performed together with primary tumor removal.

In this study, we explored the potential of FMI using cetuximab-800CW for discrimination between pathologically positive and negative LNs prior to histopathological examination. The LNs were harvested as part of a clinical trial for resection margin assessment in OSCC patients (NCT03134846) *(10)*.

METHODS

Clinical trial design

This prospective, cross-sectional, single-center diagnostic study was performed at the University Medical Center Groningen. The study is a retrospective ad hoc analysis of a clinical trial for resection margin evaluation (NCT02415881) *(10)*. Approval for the clinical trial was obtained at the Institutional Review Board of the University Medical Center Groningen (METc 2016/395). The study was performed following the Dutch Act on Medical Research involving Medical Subjects and the Helsinki Declaration (adapted version 2013, Fortaleza, Brazil). Written informed consent was obtained from all patients prior to any study-related procedure.

Study population

Patients with biopsy-confirmed OSCC which were scheduled for surgical removal of the tumor with concurrent neck dissection, were eligible for inclusion in this study. Patients were excluded from this study if they presented with a life expectancy of <12 weeks, Karnofsky performance status <70%, history of infusion reactions to monoclonal antibody therapies, QT prolongation on screening electrocardiogram, uncontrolled medical conditions or episodes within six months prior to enrollment (including uncontrolled hypertension, cerebrovascular accident, significant cardiopulmonary and liver disease), pregnancy, abnormal electrolyte status, use of class IA or III antiarrhythmic drug, or administration of an investigational drug within 30 days prior to the infusion of cetuximab-800CW.

Synthesis of cetuximab-800CW

Cetuximab-800CW was produced in the Good Manufacturing Practice facility of the University Medical Center Groningen, as previously described *(13)*. In short, cetuximab (Erbitux®) was conjugated to IRDye800CW (LI-COR Biosciences Inc., Lincoln, NE, USA) and purified using PD-10 desalting columns (Cytiva Life Sciences, Chicago, IL, USA) under controlled conditions. Cetuximab-800CW was formulated in a sodium-phosphate buffer at a concentration of 1.0 mg/mL.

Study procedures

The complete study workflow is summarized in Figure 1. Patients enrolled in the study received an unlabeled dose of 75 mg cetuximab by slow infusion, followed by a bolus injection of 15 mg cetuximab-800CW two days prior to surgery to ensure optimal primary tumor visualization *(10)*. All patients underwent tumor surgery with concurrent neck dissection according to standard of care. After surgery, neck dissection specimens were transferred to the Department of Pathology and formalin-fixed for at least 24 hours. Identification of LNs was performed by visual and tactile inspection of the neck dissection specimen. LNs were bisected when large enough and subsequently collected in cassettes. Single LNs were imaged in a closed-field fluorescence imaging system (Pearl Trilogy®, LI-COR BioSciences, Lincoln, NE, USA) at the 800 nm channel, with the center cutting plane (i.e. inner side of the LN) faced towards the camera. Regions of interest were drawn around the entire tissue specimen included in the cassette, prior to microscopic assessment.

According to standard of care, tissue was embedded in paraffin, and 4 µm tissue sections were cut of all formalin-fixed paraffin-embedded tissue blocks and then stained with hematoxylin and eosin (H&E). After routine tissue processing, we performed fluorescence flatbed scanning of these tissue blocks (Odyssey® CLx, LI-COR Biosciences, Lincoln, NE, USA). EGFR immunohistochemistry was performed of LNs from patients harboring metastases to correlate fluorescence localization with histology. A head and neck pathologist, blinded for the results of FMI, analyzed all tissue sections for the presence of tumor cells and immunohistochemistry results.

Statistical analysis

Statistical analyses and graph designs were performed using GraphPad Prism (version 9.0, GraphPad Software Inc, San Diego, CA, USA). Descriptive statistics were performed on patient demographics. Mean fluorescence intensities (FI_{mean}; arbitrary units (a.u.)) and maximal fluorescence intensities (FI_{max}; a.u.) of all LNs were calculated in ImageJ (Fiji, version 2.0.0) from the images obtained with the Pearl Trilogy®. FI_{mean} was defined as total counts per region of interest pixel area (signal/pixel). FI_{max} was defined as the

highest count measured within an region of interest pixel area. To improve the readability of the manuscript, fluorescence intensities were multiplied by 10^2. Data were tested for Gaussian distribution using Shapiro-Wilk and Anderson-Darling tests; none of the data was normally distributed. We used the Mann-Whitney U test for statistical analysis of data; all data were unpaired. Correlations were measured using Spearman's rank correlation coefficient. Cut-off values were determined based on Youden's index. Data were presented as median with range or interquartile range (IQR). Statistical significance was determined as a p-value of <0.05.

RESULTS

Between January 2019 and February 2020, 22 patients were enrolled in this study. In total, 21 patients received the study drugs consisting of an unlabeled dose of 75 mg cetuximab followed by 15 mg cetuximab-800CW two days prior to surgery. One patient developed an adverse reaction during the unlabeled cetuximab administration and was therefore excluded from the study. All remaining 21 patients completed the imaging protocol. The study procedures are summarized in Figure 1. Preoperative radiographic imaging (computed tomography and/or magnetic resonance imaging) was performed in all patients according to standard of care. Thirteen out of 21 (61.9%) patients were staged as cN0, two (9.5%) as cN1, four (19.0%) as cN2, and two (9.5%) as cN3. Five patients presented with extranodal extension. A total of 14 elective neck dissections and 12 therapeutic neck dissection were performed, with five patients undergoing bilateral neck dissection. A total of 733 specimens considered to involve a LN were submitted for processing and subsequent microscopic analysis. Of these, 145 specimens were excluded because inking of the neck dissection specimen interfered with fluorescence imaging, resulting in a total of 588 specimens suitable for analysis. 514 of these 588 specimens included LNs based on final histopathology. The remaining 74 specimens contained no LNs. 239 LNs were imaged after bisection, and 275 were imaged intact. Specimen and patient characteristics are shown in Table 1.

Differentiation between pathologically positive and negative lymph nodes

All specimens that were clinically considered as LNs (n=588) were imaged after formalin fixation and prior to histopathological examination. Six of 21 patients were diagnosed with LN metastasis upon final histopathology, with a total of 61 pathologically positive LNs. Two parameters were measured during fluorescence imaging, FI_{mean} and FI_{max}. At least a threefold increase in both FI_{max} and FI_{mean} was found in pathologically positive LNs (n=61) compared to negative LNs (n=453) or non-LN adipose or connective tissue (non-LNs) (n=74) (Fig. 2A,B). The FI_{max} of pathologically positive LNs was 2.19 (IQR 1.68-2.71) a.u. compared to 0.57 (IQR 0.39-0.80) a.u. in negative LNs ($p<0.0001$) and 0.51 (IQR 0.36-0.65) a.u. in non-LNs ($p<0.0001$), respectively (Fig. 2C). FI_{mean} was 0.92 (IQR 0.73-1.20) a.u in pathologically positive LNs versus 0.22 (IQR 0.14-0.33) a.u. in negative LNs ($p<0.0001$) and 0.21 (IQR 0.13-0.32) a.u. in non-LNs ($p<0.0001$), respectively (Supplementary Fig. 1A).

The impact of lymph node bisection on fluorescence intensity

During pathology processing, LNs were bisected if large enough and imaged with the center cutting plane (i.e. inner side of the LN) faced towards the camera. Bisected LNs showed higher fluorescence intensity compared to intact LNs (Fig. 2A,B and Supplementary Fig. 1A). Within pathologically positive LNs, bisected LNs (n=44) showed an FI_{max} of 2.39 (IQR 1.81-3.01) a.u and FI_{mean} of 1.02 (IQR 0.77-1.29) compared to an FI_{max} 1.63 (IQR 1.42-2.12) and FI_{mean} of 0.78 (IQR 0.62-0.93) a.u in nonbisected LNs (n=17) ($p=0.0013$ and 0.031, respectively). In pathologically negative LNs, bisected LNs (n=195) an FI_{max} of 0.71 (IQR 0.51-1.04) and FI_{mean} of 0.26 (IQR 0.18-0.41) were observed compared to an FI_{max} of 0.48 (IQR 0.36-0.68) and FI_{mean} of 0.19 (IQR 0.12-0.29) in nonbisected LNs (n=258) (both $p<0.0001$). In addition, body surface area showed a low correlation with FI_{max} ($R=-0.44$, $p=0.048$) but not with FI_{mean} ($R=-0.37$, $p=0.103$) in bisected pathologically negative LNs. The correlation between body surface area and FI_{max} ($R=-0.64$, $p=0.002$) and FI_{mean} ($R=-0.57$, $p=0.011$) was moderate in nonbisected pathologically negative LNs.

The impact of lymph node size and tumor volume on fluorescence intensity

Topographic studies show that metastatic tumor does not always involve the largest node within a neck dissection specimen *(14)*, emphasizing the need to develop a tool that can also detect small metastases. First, to study the impact of LN size on fluorescence intensity, we correlated diameter of pathologically negative LNs with both FI_{max} and FI_{mean}. In all LNs (n=514), a weak correlation was found between LN diameter and the FI_{max} (R=0.239, p<0.0001) and FI_{mean} (R=0.334, p<0.0001). Subsequently, in pathologically positive LNs, we studied the impact of total tumor surface area and viable tumor surface area (i.e. total tumor surface area minus necrosis surface area) on fluorescence intensity. A moderate correlation was found between total tumor surface area and FI_{max} (R=0.65, p<0.0001) and FI_{mean} (R=0.52, p<0.0001). Viable tumor surface area also showed a moderate correlation with FI_{max} (R=0.64, p<0.0001) and FI_{mean} (R=0.53, p<0.0001).

Fluorescence molecular imaging improves the efficacy of lymph node evaluation and identifies additional metastases

Next, we evaluated if FMI can discriminate between benign LNs and LNs containing metastasis. To mimic the clinical situation, we included all tissue fragments submitted to the pathologist (i.e. including non-LNs) in the analysis. Based on Youden's index, the cut-off value rendered for FI_{max} was 1.048 a.u., resulting in 100% sensitivity, 86.8% specificity, 48.9% PPV, 100% NPV and 88.2% accuracy, with an area under the curve (AUC) of 0.975 (Table 2, Fig. 2D). As such, the FI_{max} cut-off allows for a 77.4% decrease in LNs requiring microscopic examination without missing LN metastasis. For FI_{mean}, the cut-off rendered was 0.508 a.u., resulting 91.8% sensitivity, 91.9% specificity, 59.6% PPV, 99.0% NPV and 91.9% accuracy, with an AUC of 0.975 (Table 2, Supplementary Fig. 1B). ROC curves for both bisected and nonbisected LNs are provided in Supplementary Figure 2.

Since FI_{max} resulted in a NPV of 100%, a random sample of 40 false positives based on FI_{max} (i.e. FI_{max} above the cut-off, pathologically tumor-negative) were additionally examined by serial sectioning according to sentinel LN protocol to trace any missed (micro) metastasis by standard of care, as previously described *(4)*. This random sample showed a median FI_{max} of 1.38 (IQR 1.27-1.62) compared to 1.34 (IQR 1.17-1.65) in the complete false positive cohort (p=0.35), and thus was considered a representative sample.

Three additional positive LNs (7.5%) were identified in two patients. In both patients, the additional positive LN(s) resulted in upstaging of the neck from pN1 to pN2b. In one patient, this would have resulted in an intensified postoperative therapy, which had not been performed based on standard of care histopathology.

Microscopic analysis of lymph nodes

To study the distribution of cetuximab-800CW at microscopic level, EGFR immunohistochemistry was performed on a selection of pathologically positive and negative LNs. No EGFR expression was found in the negative LNs. In positive LNs, variable expression of EGFR was observed. Although EGFR expression co-localized with fluorescent signal, tumor regions without EGFR expression also showed high fluorescence, suggesting that tumor-specific fluorescence signal is not only mediated by EGFR expression (Fig. 3).

To explain this observation in the fluorescent signal distribution, H&E stained sections of pathologically positive LNs were further analyzed. Heterogeneous fluorescence intensities were observed between different tumor deposits. Within tumor deposits, we observed higher fluorescence signal in the periphery of tumor deposits compared to the center, which is in concordance with previous studies *(15)*. Generally, we observed increased fluorescent signal in regions with high tumor cell density and poor differentiation. Regions with abundant desmoplastic stroma or keratinization, associated with low cellularity, showed very low fluorescence intensities. Lastly, in necrotic areas, no fluorescence signal was observed.

Fluorescence false positive LNs were examined microscopically. As mentioned before, three (7.5%) additional metastases were detected. In other fluorescence false positives, we consistently found high vascularization compared to true negative LNs, specifically co-localizing with areas showing high fluorescence intensity at fluorescence flatbed scanning.

DISCUSSION

This study demonstrates that EGFR-targeted FMI based on intravenously administered cetuximab-800CW can be used to discriminate pathologically positive LNs from negative LNs. A cut-off value of 1.048 a.u. for FI_{max} resulted in the detection of positive LNs with 100% sensitivity and 100% NPV. Therefore, FMI can safely reduce the number of LNs requiring histopathological examination by 77.4% and improve the efficiency of pathology processing without missing any metastasis. Importantly, FMI detected pathologically positive LNs in 7.5% of the initial fluorescence false positive LNs, which were missed by standard of care histopathology. As the pathological stage of the neck often drives recommendations for postoperative therapy strategy, this could have a major impact on the adequacy of postoperative treatment and, therefore, prognosis.

Previously, EGFR-targeted FMI for the detection of LN metastasis in OSCC patients prior to formalin-fixation has been evaluated *(16, 17, 18)*. In dose-escalation studies with cetuximab-800CW and panitumumab-800CW, tumor-positive LNs were identified with high sensitivity, although a dose-dependent increase in false fluorescence positive LNs was observed *(17, 18)*. In one study, they showed that signal-to-noise ratio and FI_{mean} could guide the *ex vivo* assessment of nodal specimens and identify tumor-positive LNs with high sensitivity and specificity *(17)*. Yet, the use of signal-to-background ratio requires knowledge of the presence and dimensions of a possible tumor, so this strategy cannot be applied to select at-risk LNs prior to histopathological evaluation. More recently, Krishnan et al. reported the use of 50 mg panitumumab-800CW administered 1-5 days prior to surgery for LN assessment. The authors found that using a fluorescence nodal ranking method, accurate nodal staging was achieved in all patients when analyzing the top 5 LNs *(16)*. This method is based on relative fluorescence intensities, so in all patients microscopic examination of LNs is required, even when low absolute fluorescence intensities are observed. Since most patients (55.6% in their cohort) have a pathologically negative neck, we believe using a FI_{max} cut-off is favorable since this rules out the necessity to examine LNs microscopically in all patients.

The uniqueness of our data compared to previous studies described lies in the use of a single dose of cetuximab-800CW being consistently administered two days prior to surgery, allowing us to propagate a reliable cut-off value for subsequent studies. We advocate the use of FI_{max} over FI_{mean} for swift clinical implementation since it does not require additional steps between imaging and selection, such as drawing regions of interest. Here, we propose using a grid to automatically identify LNs based on the FI_{max} measured in each square of the grid (Fig. 4). This method enables user-friendly evaluation of all harvested LNs within minutes while reducing the LNs requiring microscopic assessment by 78.0%.

Although these results are promising for clinical use, our study has some limitations. Despite the use of a low dose of cetuximab-800CW that empirically would decrease the number of false positives *(17, 18)*, our dosing strategy was optimized for margin assessment of the primary tumor rather than evaluating LNs. Secondly, although we observed high fluorescence intensity in all regions showing EGFR expression, high fluorescence intensities were also found in regions without EGFR expression. This varying co-localization was also described earlier by Nishio et al. *(17)* and coincides with other studies that found that EGFR expression did not correlate with cetuximab uptake in PET imaging *(19, 20)*, nor could predict response to cetuximab therapy *(21, 22, 23)*. The significance of EGFR staining is questionable, as it has been shown that EGFR expression as determined by immunohistochemistry does not solely reflect tumor biology *(24)*.

As such, we hypothesize that additional mechanisms within the tumor microenvironment influence accumulation of cetuximab-800CW, and the presence of EGFR may not be the only determinant, which has also been observed in EGFR-targeted photodynamic therapy *(25, 26)*. Multiple studies on FMI and other imaging modalities have pointed out the role of vascularization and interstitial pressure in the accumulation of targeted contrast agents *(15, 19, 23)*. This does also fit the observation that the fluorescence false positives in the current study showed aberrant vascularization, possibly leading to the accumulation of cetuximab-800CW through the enhanced permeability and retention effect.

In future, studies could evaluate new dosing strategies dedicated to the assessment of LNs. For example, adding a second, untargeted tracer with different spectral properties. This would enable correction for nonspecific tracer accumulation and increases the contrast between tumor tissue and non-tumor tissue within LNs *(27)*. This enhanced contrast may further increase the accuracy of FMI for postoperative LN assessment. Secondly, we hypothesize that these FMI results can be translated to the assessment of freshly excised LN specimens , albeit fresh LNs may show slightly different fluorescence intensities no formalin fixation is performed prior to imaging. This may impact the signal due to the wash out of nonspecific fluorescent tracer or alteration of tissue optical properties *(28, 29)*. Here, the intraoperative use of FMI depends on the surgical procedure of the neck. Intraoperative LN biopsies allow for immediate intraoperative imaging since single LNs are excised. However, FMI could also be used for the analysis of an elective neck dissection specimen, although this is logistically more challenging since it requires intraoperative fluorescence analysis of LNs by a second clinician (e.g. pathologist or lab technician). The intraoperative identification of a tumor-positive LN enables direct extension to a therapeutic neck dissection is possible, which may prevent second surgery. This eventually will decrease both patient burden and healthcare costs by reducing operation time.

In conclusion, our findings suggest that FMI with the intravenously administered EGFR-targeting fluorescent tracer cetuximab-800CW, can aid in the detection of LN metastases in the *ex vivo* setting in OSCC patients. We demonstrate that this method can improve the efficiency of postoperative LN assessment without missing LN metastases. Importantly, FMI may identify additional LN metastases, leading to more accurate staging of the neck and appropriate postoperative treatment, which may eventually improve prognosis.

ACKNOWLEDGEMENTS

To all patients who participated in this study. Rachel Dopheide, Hilde Bouma-Boomsma and Karien Kreeft-Polman for their help in recruiting patients. Erik Bleuel, Maaike Barentsen and Lilo Janssens.

for the assistance during tissue processing.

DISCLOSURES

GMvD is CEO, founder and shareholder of TRACER Europe BV / AxelaRx. BvdV is member of the Scientific Advisory Board of Visiopharm for which compensation is received by the University Medical Center Groningen. The other authors declare no conflict of interest.

FUNDING

This research was funded by the Dutch National Cancer Society (RUG 2015-8084).

KEY POINTS

Question: Can EGFR-targeted fluorescence molecular imaging differentiate between tumor-positive and tumor-negative lymph nodes?

Pertinent findings: In this retrospective ad hoc analysis, we show that the preoperative intravenously administered cetuximab-800CW can detect tumor-positive lymph nodes *ex vivo* with 100% sensitivity and 86.8% specificity (AUC 0.97). Additionally, in 7.5% of the 38 fluorescence false positive lymph nodes, we identified additional metastasis missed by standard of care.

Implications for patient care: This image-guided concept may improve the efficacy of lymph node processing while detecting additional metastases, which safeguards appropriate postoperative therapy and may improve patient prognosis.

REFERENCES

1. Ho AS, Kim S, Tighiouart M, et al. Metastatic lymph node burden and survival in oral cavity cancer. *J Clin Oncol*. 2017;35:3601-3609.

2. Divi V, Chen MM, Nussenbaum B, et al. Lymph node count from neck dissection predicts mortality in head and neck cancer. *J Clin Oncol*. 2016;34:3892-3897.

3. Weiss MH, Harrison LB, Isaacs RS. Use of decision analysis in planning a management strategy for the stage N0 neck. *Arch Otolaryngol Head Neck Surg*. 1994;120:699-702.

4. Boeve K, Schepman KP, Schuuring E, et al. High sensitivity and negative predictive value of sentinel lymph node biopsy in a retrospective early stage oral cavity cancer cohort in the northern netherlands. *Clin Otolaryngol*. 2018. Epub ahead of print.

5. Woolgar JA, Triantafyllou A. Lymph node metastases in head and neck malignancies: Assessment in practice and prognostic importance. *Diagn Histopathol*. 2010;16:265-275.

6. Weissleder R. A clearer vision for in vivo imaging. *Nat Biotechnol*. 2001;19:316-317.

7. Koch M, Ntziachristos V. Advancing surgical vision with fluorescence imaging. *Annu Rev Med*. 2016;67:153-164.

8. Koch M, Symvoulidis P, Ntziachristos V. Tackling standardization in fluorescence molecular imaging. *Nat Photonics*. 2018;12:505-515.

9. Grandis JR, Tweardy DJ. TGF-alpha and EGFR in head and neck cancer. *J Cell Biochem Suppl*. 1993;17F:188-191.

10. Voskuil FJ, de Jongh SJ, Hooghiemstra WTR, et al. Fluorescence-guided imaging for resection margin evaluation in head and neck cancer patients using cetuximab-800CW: A quantitative dose-escalation study. *Theranostics*. 2020;10:3994-4005.

11. Gao RW, Teraphongphom NT, van den Berg NS, et al. Determination of tumor margins with surgical specimen mapping using near-infrared fluorescence. *Cancer Res*. 2018;78:5144-5154.

12. Vonk J, de Wit JG, Voskuil FJ, Witjes MJH. Improving oral cavity cancer diagnosis and treatment with fluorescence molecular imaging. *Oral Dis*. 2021;27(1):21-26.

13. Linssen MD, Ter Weele EJ, Allersma DP, et al. Roadmap for the development and clinical translation of optical tracers cetuximab-800CW and trastuzumab-800CW. *J Nucl Med*. 2019;60:418-423.

14. Woolgar JA. Detailed topography of cervical lymph-note metastases from oral squamous cell carcinoma. *Int J Oral Maxillofac Surg*. 1997;26:3-9.

15. Lu G, Fakurnejad S, Martin BA, et al. Predicting therapeutic antibody delivery into human head and neck cancers. *Clin Cancer Res*. 2020;26:2582-2594.

16. Krishnan G, van den Berg NS, Nishio N, et al. Metastatic and sentinel lymph node mapping using intravenously delivered panitumumab-IRDye800CW. *Theranostics*. 2021;11:7188-7198.

17. Nishio N, van den Berg NS, van Keulen S, et al. Optical molecular imaging can differentiate metastatic from benign lymph nodes in head and neck cancer. *Nat Commun*. 2019;10:5044-019-13076-7.

18. Rosenthal EL, Moore LS, Tipirneni K, et al. Sensitivity and specificity of cetuximab-IRDye800CW to identify regional metastatic disease in head and neck cancer. *Clin Cancer Res*. 2017;23:4744-4752.

19. Aerts HJ, Dubois L, Perk L, et al. Disparity between in vivo EGFR expression and 89Zr-labeled cetuximab uptake assessed with PET. *J Nucl Med*. 2009;50:123-131.

20. van Helden E, Elias S, Gerritse S, et al. [89 zr] zr-cetuximab PET/CT as biomarker for cetuximab monotherapy in patients with RAS wild-type advanced colorectal cancer. *European Journal of Nuclear Medicine and Molecular Imaging*. 2019:1-11.

21. Driehuis E, Kolders S, Spelier S, et al. Oral mucosal organoids as a potential platform for personalized cancer therapy. *Cancer Discov*. 2019;9:852-871.

22. Bossi P, Resteghini C, Paielli N, Licitra L, Pilotti S, Perrone F. Prognostic and predictive value of EGFR in head and neck squamous cell carcinoma. *Oncotarget*. 2016;7:74362-74379.

23. Even AJ, Hamming-Vrieze O, van Elmpt W, et al. Quantitative assessment of zirconium-89 labeled cetuximab using PET/CT imaging in patients with advanced head and neck cancer: A theragnostic approach. *Oncotarget*. 2017;8:3870-3880.

24. Chung KY, Shia J, Kemeny NE, et al. Cetuximab shows activity in colorectal cancer patients with tumors that do not express the epidermal growth factor receptor by immunohistochemistry. *J Clin Oncol*. 2005;23:1803-1810.

25. van Driel PBAA, Boonstra MC, Slooter MD, et al. EGFR targeted nanobody-photosensitizer conjugates for photodynamic therapy in a pre-clinical model of head and neck cancer. *J Control Release*. 2016;229:93-105.

26. Peng W, de Bruijn HS, Farrell E, et al. Epidermal growth factor receptor (EGFR) density may not be the only determinant for the efficacy of EGFR-targeted photoimmunotherapy in human head and neck cancer cell lines. *Lasers Surg Med*. 2018;50:513-522.

27. Tichauer KM, Samkoe KS, Gunn JR, et al. Microscopic lymph node tumor burden quantified by macroscopic dual-tracer molecular imaging. *Nat Med*. 2014;20:1348-1353.

28. Samkoe KS, Sardar HS, Bates BD, et al. Preclinical imaging of epidermal growth factor receptor with ABY-029 in soft-tissue sarcoma for fluorescence-guided surgery and tumor detection. *J Surg Oncol*. 2019;119:1077-1086.

29. Kapoor S, Lu G, van den Berg, Nynke S, et al. Effect of formalin fixation for near-infrared fluorescence imaging with an antibody-dye conjugate in head and neck cancer patients. *Mol Imaging Biol*. 2021;23(2):270-276

TABLES AND FIGURES:

Table 1: Patient demographics and tumor characteristics of all patients

	pN+ n = 7	pN- n = 14	All patients n = 21
Median age (range)	67 (65-82)	64 (29-78)	66 (29-82)
Female, n (%)	6 (85.8)	8 (57.1)	14 (67.7)
Median weight (range), kg	73 (52-105)	84 (53-140)	80 (52-140)
Median BSA (range), m^2	1.87 (1.52-2.17)	1.99 (1.58-2.67)	1.96 (1.52-2.67)
LNs, n (%)	261	358	619
Level I	49 (18.8)	72 (20.1)	121 (19.5)
Level II	50 (19.2)	102 (28.5)	152 (24.6)
Level III	74 (28.4)	121 (33.8)	195 (31.5)
Level IV	58 (22.2)	47 (13.1)	105 (17.0)
Level V	30 (11.5)	16 (4.5)	46 (7.4)
Positive LNs[#], n (%)	64	NA	64
Level I	5 (7.8)		5 (7.8)
Level II	11 (17.2)		11 (17.2)
Level III	19 (29.7)		19 (29.7)
Level IV	19 (29.7)		19 (29.7)
Level V	10 (15.6)		10 (15.6)
Patients with ENE, n (%)	5 (62.5)	NA	5 (23.8)
pN-stage, n (%)[#]			
N0	0 (0)	14 (100)	14 (66.7)
N1	2 (28.6)	0	2 (9.5)
N2	4 (81.6)	0	4 (19.0)
N3	1 (20.4)	0	1 (4.8)
pT-stage, n (%)			
T1	1 (14.3)	5 (35.7)	6 (28.6)
T2	2 (28.6)	3 (21.4)	5 (23.8)
T3	1 (4.8)	0	1 (4.8)
T4	3 (42.9)	6 (42.9)	9 (42.9)
Neck dissection, n (%)*			
Elective	11 (64.7)	3 (33.3)	14 (53.8)
Therapeutic	6 (35.3)	6 (66.7)	12 (46.2)

BSA, body surface area. LN, lymph node. pN, pathological nodal stage. pT, pathological tumor stage. [#]Initially, six patients were diagnosed with a pathologically positive neck. Since three additional metastases were found based on FMI (see section *'Microscopic analysis of lymph nodes'*), a total of 64 tumor-positive LNs was found, and one patients was upstaged from a pN0 to a pN1. *Five patients received a bilateral neck dissection and therefore the total number of neck dissections equals 26.

Table 2: Performance of fluorescence imaging using cetuximab-800CW at the optimal cut-off value for selection of at-risk lymph nodes.

Cut-off	Sensitivity (%)	Specificity (%)	PPV (%)	NPV (%)	Accuracy (%)	Preselected LNs (%)
FI_{max} ≥1.048	100.0%	86.8%	48.9%	100.0%	88.2%	22.6%
FI_{mean} ≥0.508	91.8%	91.9%	59.6%	99.0%	91.9%	17.2%

Based on receiver operating curves (ROC), the optimal fluorescence intensity cut-offs were determined to discriminate between positive LNs and negative LNs. Here, 100% sensitivity and NPV were used as main criteria for the use of FMI as a selection tool for the pathologist. Missing LN metastases should be avoided since appropriate postoperative therapy is essential to provide optimal prognosis. Abbreviations: LN, lymph node; $FI_{max,}$ maximum fluorescence intensity; FI_{mean}, mean fluorescence intensity; FMI, fluorescence molecular imaging; PPV, positive predictive value; NPV, negative predictive value.

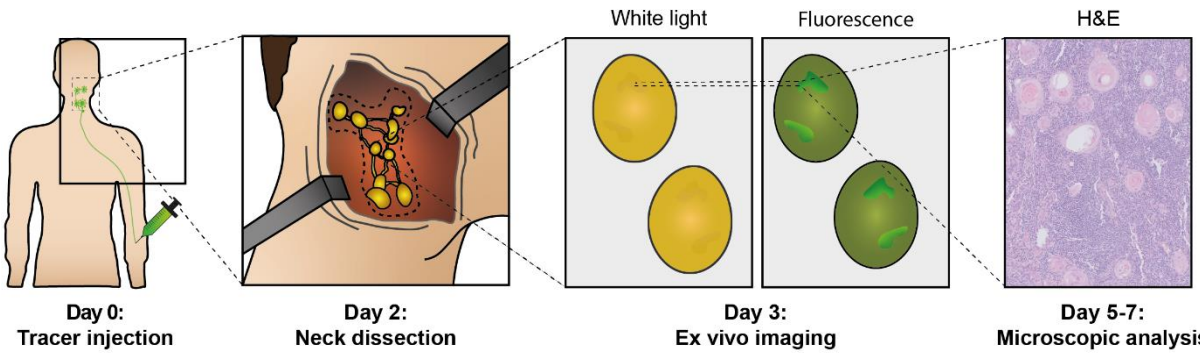

402

403 **Figure 1: Summary of study workflow.** All patients were administered with the fluorescent tracer
404 cetuximab-800CW intravenously two days prior to surgery. After primary tumor surgery and neck
405 dissection, nodal specimens were submitted to the Department of Pathology and subsequently fixated in
406 formalin for at least 24 hours. All formalin-fixed tissue that could involve a LN was imaged in a closed-
407 field imaging system and submitted for standard of care microscopic evaluation to correlate fluorescence
408 signal with H&E histopathology. Abbreviations: H&E, hematoxylin and eosin.

409

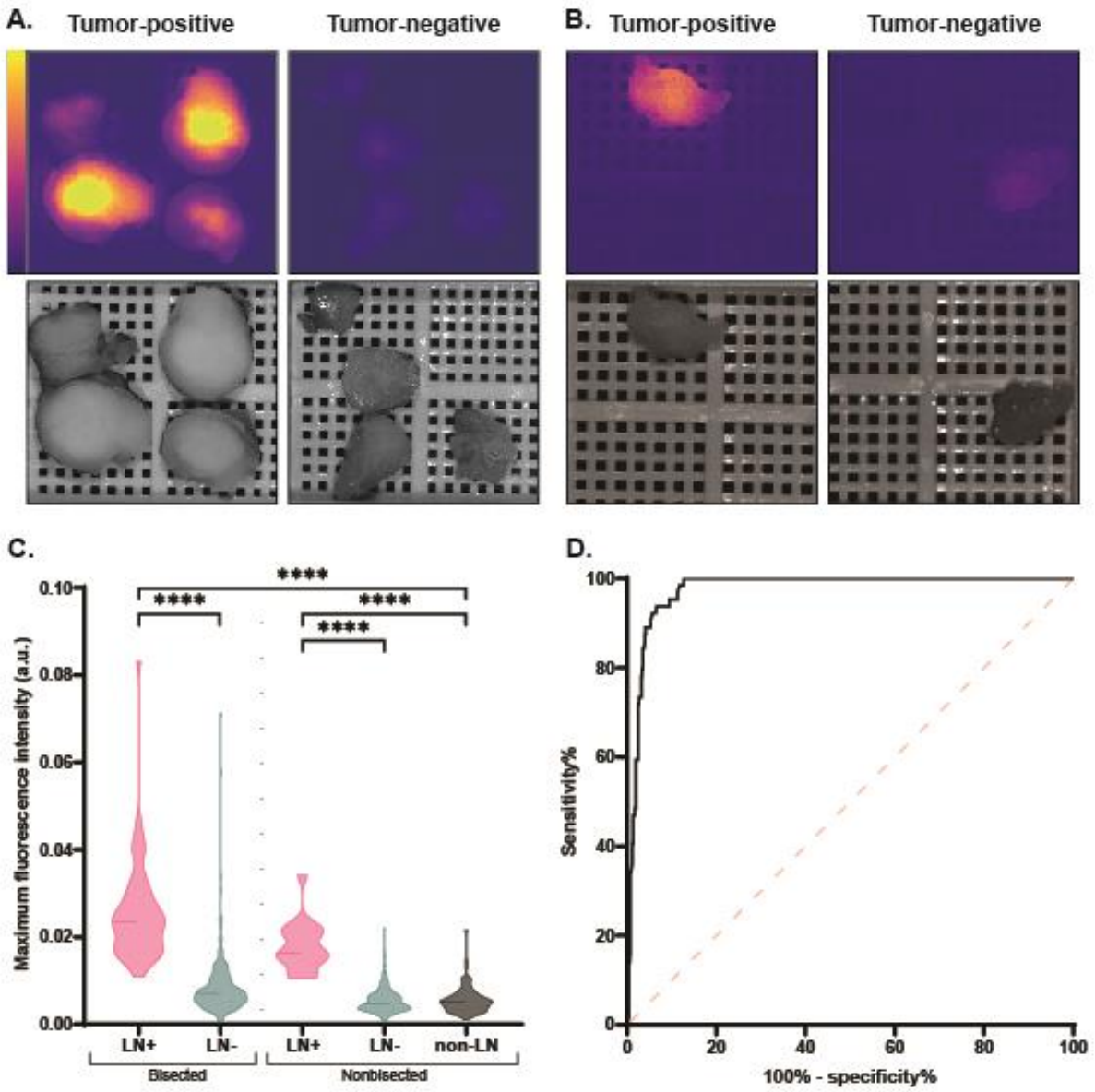

Figure 2: Fluorescence molecular imaging with cetuximab-800CW enables discrimination between positive and negative lymph nodes. A,B) Representative images of bisected (A) and nonbisected (B) pathologically positive and negative formalin-fixed LNs from a subject that was diagnosed with metastases upon final histopathology. Increased fluorescence intensity was observed in both bisected and nonbisected pathologically positive LNs compared to pathologically negative LNs. **C)** The FI_{max} is significantly increased in pathologically positive LNs compared to negative LNs and non-LNs, respectively****, both in bisected and nonbisected LNs (all $p<0.0001$). **D)** ROC curve based FI_{max} shows a high area under the curve

of 0.975. LN, lymph node; FI_{max}, maximum fluorescence intensity; ROC, receiver operating characteristic; ****: p<0.0001

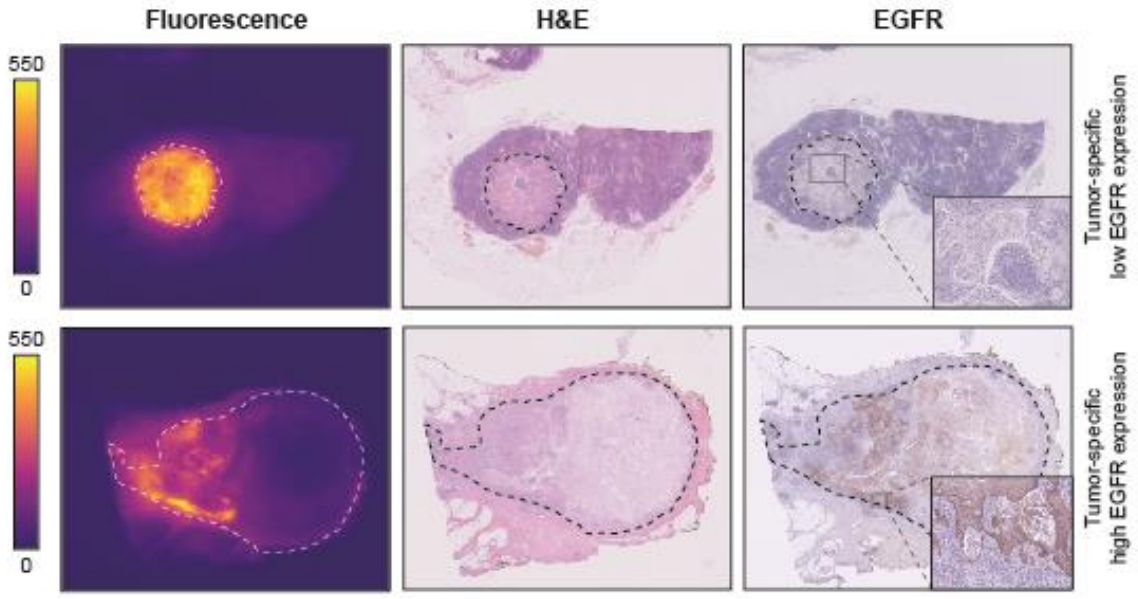

Figure 3: Microscopic analysis. Representative images of formalin-fixed lymph node metastases that were diagnosed upon final histopathology. On both the fluorescence images and H&E slide, the tumor region is delineated with a dashed line. Fluorescence flatbed scanning shows increased fluorescence intensity in tumor-deposits compared to adjacent lymphoid and connective tissue. Although EGFR expression is variable within patients, the fluorescence signal is tumor-specific, suggesting that other mechanisms play a role in cetuximab-800CW accumulation. H&E, hematoxylin and eosin; EGFR, epidermal growth factor receptor.

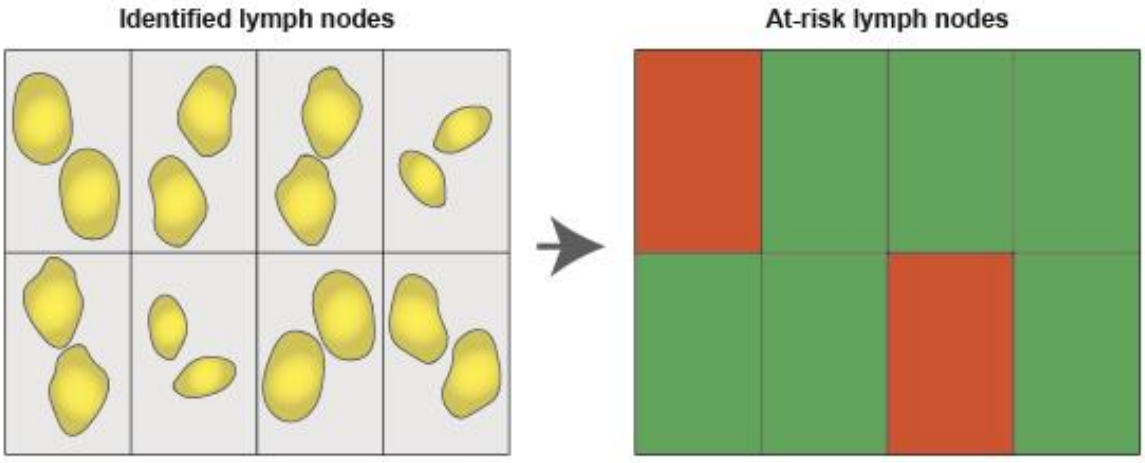

Figure 4: Grid selection of lymph nodes for microscopic evaluation. Using a grid, fluorescence imaging of identified lymph nodes can automatically identify the lymph nodes that display a FI_{max} above the set cut-off. In contrast to FI_{mean}, this approach does not require drawing a region of interest around the lymph nodes. As such, at-risk lymph nodes can be selected rapidly without interfering with standard of care. FI_{max}, maximum fluorescence intensity; FI_{mean}, mean fluorescence intensity.

Graphical Abstract

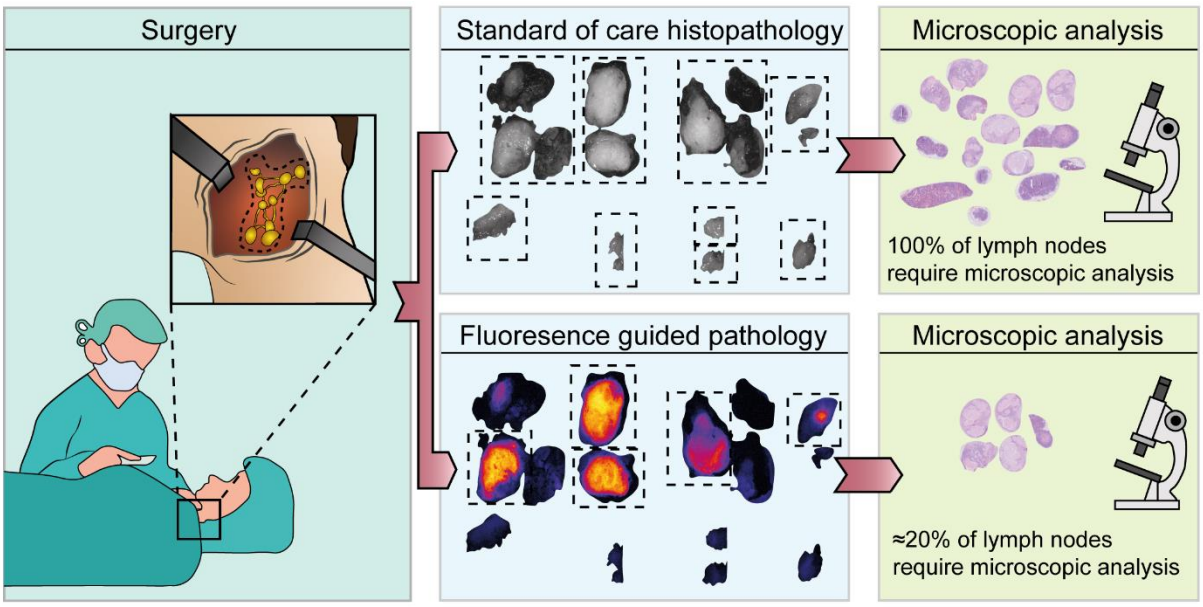

SUPPLEMENTARY FIGURES

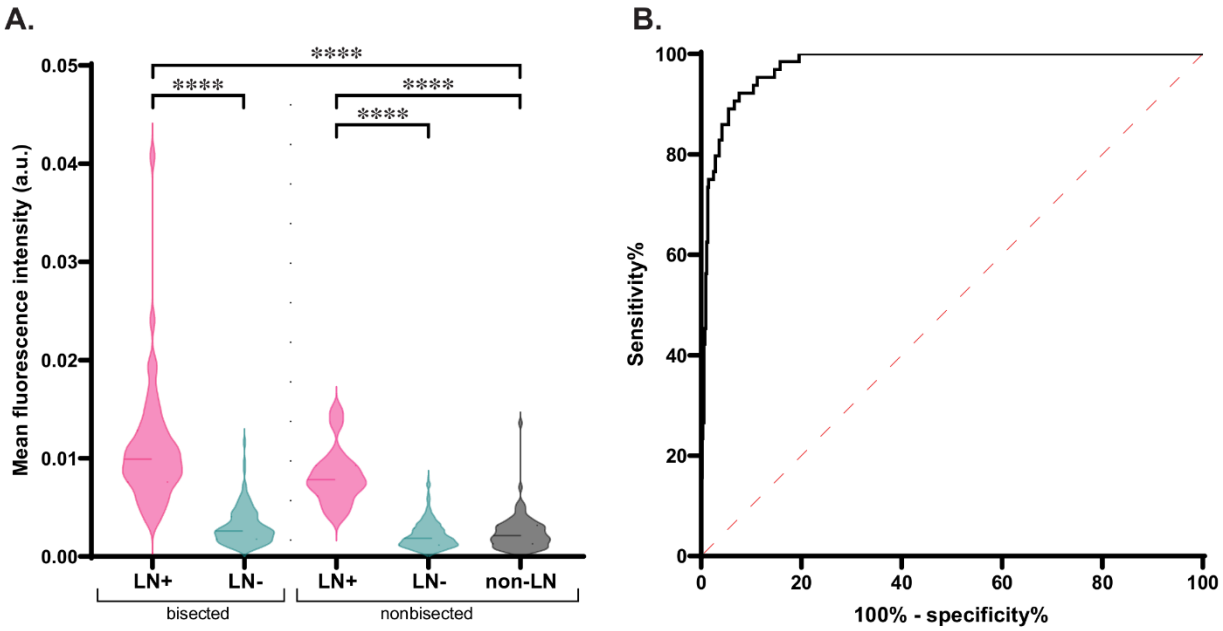

Figure S1: Mean fluorescence intensity to discriminate between pathologically positive and negative lymph nodes. A) The MFI is significantly increased in pathologically positive LNs compared to negative LNs and non-LNs containing tissue****, both in bisected and nonbisected LNs (all p<0.0001). **B)** ROC curve based MFI shows a high area under the curve of 0.976. LN, lymph node; MFI, mean fluorescence intensity; ROC, receiver operating characteristic. ****: p<0.0001

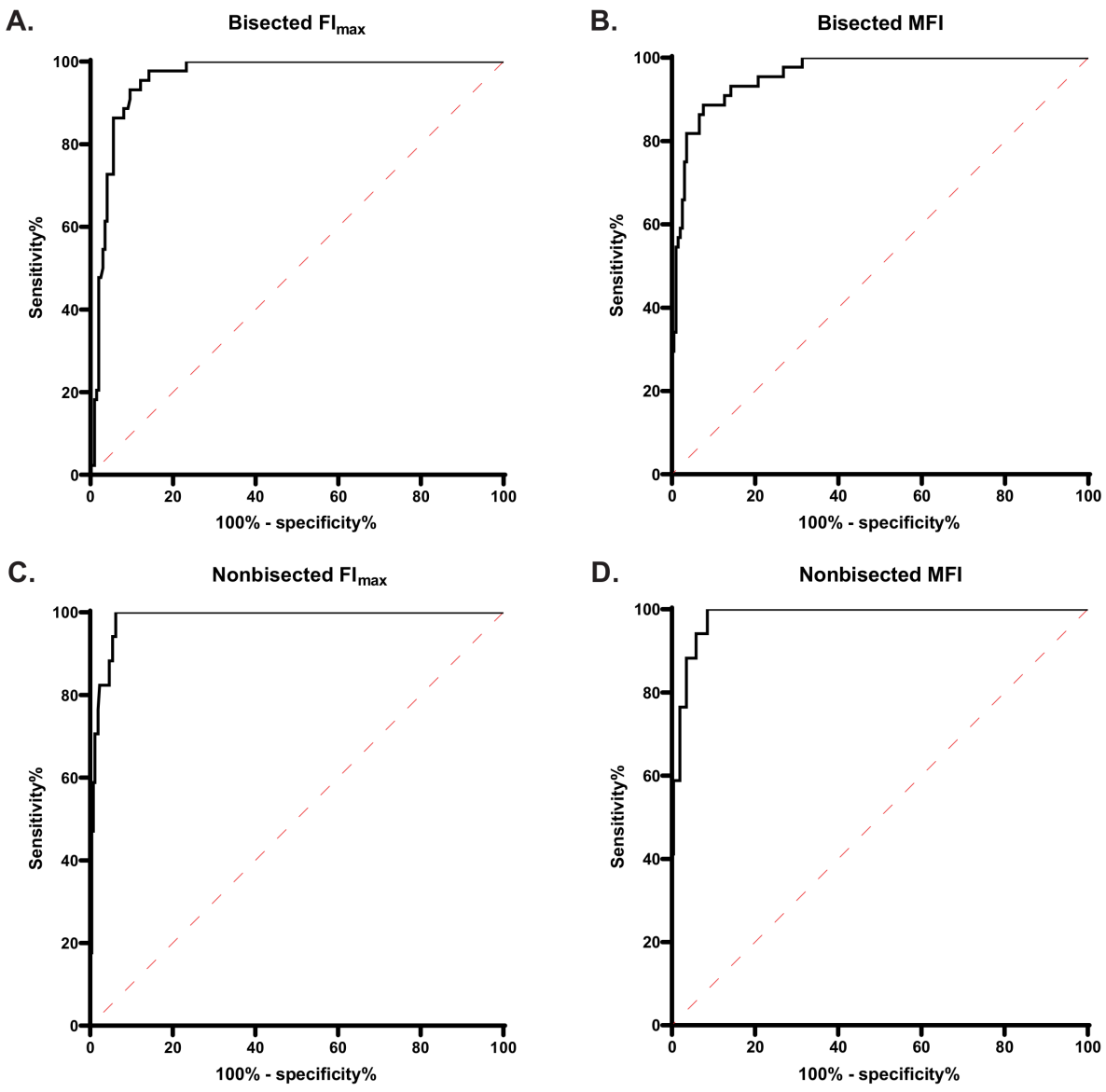

Figure S2: ROC curves of bisected and nonbisected lymph node imaging. A,B) ROC curves of bisected LNs based on FI_{max} and MFI showing an AUC of 0.959 and 0.961, respectively. **C,D)** ROC curves of nonbisected LNs based on FI_{max} and MFI showing an AUC of 0.985 and 0.983, respectively.